

Article

Simulated Prediction of Roof Water Breakout for High-Intensity Mining under Reservoirs in Mining Areas in Western China

Tao Yang ^{1,*}, Jiayue Deng ¹, Bing Peng ², Jie Zhang ¹, Yiming Zhang ¹ and Yihui Yan ¹

¹ College of Energy, Xi'an University of Science and Technology, Xi'an 710054, China; djiy1085059714@163.com (J.D.); zhangj@xust.edu.cn (J.Z.); 22203226066@stu.xust.edu.cn (Y.Z.); 21203226039@stu.xust.edu.cn (Y.Y.)

² Shaanxi Province Mineral Resources Investigation and Evaluation Center, Xi'an 710054, China; pengbingdizhi@sina.cn

* Correspondence: yangtao@xust.edu.cn; Tel.: +86-186-8296-6978

Abstract: China is rich in coal resources under water bodies. However, the safety prediction of high-intensity mining under water bodies has long been one of the problems encountered by the coal industry. It is of great significance to realize safe mining under water bodies, improve the recovery rate of coal resources and protect reservoir resources. Therefore, this article takes the No. 5 coal seam and No. 11 mining area of the Wangwa Coal Mine as the research object, and integrates physical simulation, numerical simulation, theoretical analysis, and other methods to study the development height of water-conducting fracture zones in fully mechanized top coal caving mining. Solid–liquid coupling physical simulation tests reveal the failure characteristics of overlying strata in goaf and the seepage law of reservoir water under the influence of mining. By comparing the monitoring data of borehole leakage, the measured data obtained by borehole monitoring with the height data of the water-conducting fracture zone obtained by the traditional empirical formula of three-under standard, the error between the two is as high as -29.39% . In this case, the variance correction coefficient is used to correct the empirical formula, and on this basis, in order to effectively protect the surface water dam and water body, the mining height of the coal seam in the working face with limited height mining is inversely derived. The research results provide a basis for the safety prediction of high-intensity mining under the reservoir dam in the ecologically fragile areas of western China and a scientific guarantee for the formulation of safety measures under such conditions.

Keywords: coal mining under reservoirs; high-intensity mining; green mining; physical simulation; water conducting fracture zone



Citation: Yang, T.; Deng, J.; Peng, B.; Zhang, J.; Zhang, Y.; Yan, Y.

Simulated Prediction of Roof Water Breakout for High-Intensity Mining under Reservoirs in Mining Areas in Western China. *Appl. Sci.* **2023**, *13*, 9902. <https://doi.org/10.3390/app13179902>

Academic Editor: Lina M. López

Received: 7 June 2023

Revised: 14 July 2023

Accepted: 17 July 2023

Published: 1 September 2023



Copyright: © 2023 by the authors. Licensee MDPI, Basel, Switzerland. This article is an open access article distributed under the terms and conditions of the Creative Commons Attribution (CC BY) license (<https://creativecommons.org/licenses/by/4.0/>).

1. Introduction

As the leading energy source in China, the safe and efficient exploitation of coal resources is a major strategic demand for China. China's "double carbon" strategic goal and the "14th Five-Year Plan and Outline of Vision Goals for 2035" clearly put forward increasing the safe and efficient utilization of coal and other fossil energy resources [1]. However, there are still a large number of coal resources under high-quality water bodies, and according to incomplete statistics, nearly 10 billion tons of coal resources are pressed under various types of water bodies in China, which seriously affects the service life of mines. Moreover, the protection of these high-quality water bodies and the safe mining of coal resources pressed under water bodies are one of the problems that need to be solved and improved in China's coal industry [2]. The disorderly development of coal will bring groundwater damage and surface ecological damage [3], so China attaches great importance to the protection of water resources in mining areas. In 2013, the National Development and Reform Commission issued the Development Plan for the Utilization of Mine Water [4] and in 2014, the State Council issued the Action Plan for the Prevention and Control of Water Pollution (Water Ten), which pointed out that to promote the comprehensive utilization

of mine water, the supplementary water in coal mines, surrounding area production and ecological water should give priority to the use of mine water [5]. The issue of mining under water bodies should not only consider safety issues, especially in the western ecologically fragile areas, but also take into account the protection of precious freshwater resources on the surface and water conservation facilities [6].

In the study of underground mining of water resources in western ecologically fragile areas, the hydraulic fissures caused by underground coal mining are the root cause of groundwater loss and surface ecological deterioration [7]. The study reveals the development pattern of mining hydraulic fissures in western mining areas, which is important for carrying out regional coal green mining [8]. Wu Qiang et al. [9] discussed the concept of dual-resource coal mine construction and development, put forward the mine groundwater control, utilization, ecological and environmental protection “trinity” optimization combination, underground water clearing and sewage diversion, surface and underground joint drainage and mine water resources, such as the construction of dual-resource coal-water mine specific technical methods. Wang Shuangming [10–12] and others evaluated the zoning of water conservation mining in terms of hydrogeological conditions and water level burial depth to target appropriate water conservation mining methods, which initially formed the basic framework of water conservation mining research. Fan Limin [13–15] and others considered that in water-scarce mining areas in western China, coal mining, water resources protection, and ecological environment safety should be developed in a coordinated way through a rational layout and scientific mining. In 2000, we also measured the fracture height of the coal seam after mining according to the consumption of flushing fluid in the borehole. Huang Qingxiang [16–18] analyzed the characteristics of the water-holding rock group in the aquifer, and he also classified water-preserving coal mining into three types, namely, natural water-preserving mining, controlled water-preserving mining, and special water-preserving mining. Chi Mingbo et al. [19] considered the resource properties of water and gave a set of evaluation systems to define and calculate the water resource carrying capacity. Zhang Jie et al. [20] used physical simulation tests to study the damage law of shallow coal seam overburden and pointed out that the mining height is the main factor affecting the development height of the water-conducting fracture zone. Lai Xingping et al. [21] used a physically similar simulation test to investigate the law of water-conducting fissure zone development in the comprehensive release working face of three soft coal seams. They discovered that the law of mining intensity on the reservoir area and periodic incoming pressure will cause an increase in water gushing at the working face. Gale W’s [22] study assessed available data of inflows into underground coal mines and utilized computer simulation of water flows through fracture networks. The study concluded that flows into mines is typically via an interconnected network of preexisting and mining-induced fractures. The height above the coal seam that mining-induced fractures extend is typically related to the width of the panel. A study by R. K. Tiwar [23] has shown the characteristics of acidic and nonacidic mine water that permeate from open pit coal mines; there is an accumulation of petroleum, oil and grease, and heavy metals in the coal mine wastewater and it is recommended to manage these waste liquids to control the level of pollution at the source.

The above research concepts of green mining and water conservation mining have an important role in the research of predicting the height of water-conducting rift zones on the roofs of coal seams, but due to the complex geological environment of mines in northwest China, the surface is covered by a thick loess layer, and the mining disturbance on the surface is intense under the geological conditions of the extra thick coal seam. This results in the significant and complicated development of water-conducting rift zones, and no reliable prediction of the height of water-conducting rift zone development in comprehensive mining has been formed so far. The research on the development height of water-conducting fracture zones under different geological conditions has always been a key research topic for mine geologists in China. Based on the above and a large number of research results, the industry has revised and compiled new specifications and guide-

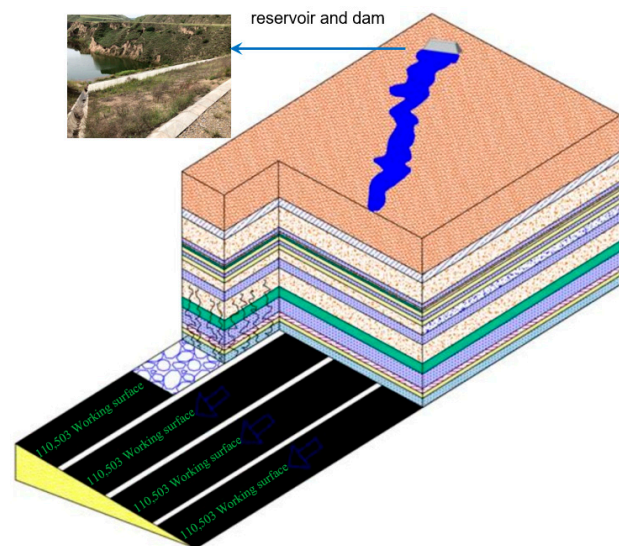
lines [24], which provide a scientific guarantee for guiding the safe mining of coal in the coal mines “under three”. From the perspective of coal production, mining under water bodies is more concerned with the safety of the coal mine itself, but often neglects the safety and normal use of the water body and hydraulic structures [25], such as mining under reservoirs, as the reservoir itself plays the role of flood control, water storage, irrigation, power generation, breeding, etc.; thus, the safety of reservoir water bodies and dams must also be given attention. In this paper, the feasibility and safety of coal seam mining under the reservoir of the Wangwa coal mine in the western ecologically fragile area of China are analyzed and discussed in the context of high-intensity mining under the dam of the mine’s pea ditch reservoir to provide a reference for safe mining under similar conditions.

2. Project Summary

The Wangwa coal mine is located in Wangwa town, Ningxia Hui Autonomous Region, Ningxia. The Wangwa coal mine is a key poverty alleviation project established by the autonomous region to solve the fuel structure in the mountainous area of Ningnan. The mine is now approved to have a production capacity of six million tons per year. It currently mines No. 5 coal, has a coal seam depth of 432.81 m, has an average coal thickness of 9.08 m, is a very thick coal seam, has a mining height of 3 m and a coal release height of 6.08 m. There is an artificial reservoir in the southwest of the well field with a total storage capacity of 770,000 m³. The reservoir is a national poverty alleviation project, which provides water for local agricultural irrigation and serves as a local humanistic landscape project. The reservoir is located within the mining area of the No. 11 mining area of the Wangwa coal mine, running through 110,503, 110,505, 110,507, and 110,509 working faces of the No. 11 mining area. A schematic diagram of the mine working face layout and stratigraphy (drawn using FLAC^{3D} version 6.0 software) is shown in Figure 1.

No.	Lithology	Histogram	Thickness/m
1	Loess		60.00
2	Sub-clay		123.90
3	Conglomerate		16.55
4	Coarse sandstone		61.35
5	Siltstone		10.00
6	Coarse sandstone		6.10
7	Mudstone		5.62
8	Fine Sandstone		12.00
9	Siltstone		7.48
10	Fine Sandstone		8.00
11	Coarse sandstone		12.04
12	Siltstone		17.89
13	Coarse sandstone		39.00
14	Mudstone		12.35
15	Siltstone		24.12
16	Carbonaceous mudstone		2.00
17	Fine Sandstone		1.18
18	Siltstone		3.00
19	Mudstone		1.23
20	5#Coal		9.08

(a)



(b)

Figure 1. Mine working face layout and strata diagram. (a) Mine working face layout diagram. (b) strata diagram.

According to the stratigraphic diagram of the working face of mining area No. 11, the surface of the mine area is covered by a thick soil layer, the roof of the coal seam is

mainly siltstone and mudstone, the lithology of the roof is good, and more horizontal laminations and small interlocking laminations are developed. Only a small amount of fine sandstone and coarse sandstone is distributed in the north with a thickness of 0.50~34.05 m and an average thickness of 4.11 m. However, because there is an artificial reservoir in the No. 11 mining area and the working face of the mine is mined by the strike longwall backward, the integrated mechanized low-level roof coal mining method is used, which are all collapse methods for managing the roof. Mining disturbances are intense, and the pattern of development of water-conducting fissure zones has not yet been explored. A similar study was carried out by A.V. Mokh [26], focusing on the permeability coefficient between the water-conducting fracture zone and the rock mass. However, there is no relevant research on this law in China. In order to ensure the safe mining of coal mines and protect the water resources of the dam, it is necessary to reasonably predict the development height of the water-conducting fracture zone of the working face and the damage degree of the dam.

3. Analysis of Fracture Evolution of High-Intensity Mining Overburden under Reservoir Dams

3.1. Experimental Design of Physical Simulation

Since the mine does not have a clear grasp of the overburden rock transport and fissure distribution under the mining conditions of 110,505 working face, and the engineering period is long and costly if the field engineering measurement is carried out blindly, the working face with similar endowment conditions and the safety hazard of water breakout are selected as the simulation prototype to conduct physical simulation experiments [27] to study the overburden rock breakout movement and fissure distribution of the high-intensity mining working face under the reservoir dam. In order to simulate the destruction characteristics of the overlying rock layer on the working surface under the 110,505 mining area and the development height of the water-conducting fracture zone, based on the solid–liquid coupling test platform [28], river sand is used as an aggregate and cement and white powder as cementing materials for the ratio test, developing nonhydrophilic solid–liquid coupling material [29], and high-precision water molecule tester, infrared imager [30], total station, and borehole monitoring are used for the top slab water influx, hydraulic fracture zone, and overburden movement. Based on the simulation test similarity theory, the parameters of coal seam depth and coal seam thickness in the simulated mining area [31], combined with the test bench geometry, the similarity constants selected for this test were divided into two parts. The similar material model parameters and material ratios are shown in Table 1, and the model design (drawn using FLAC^{3D} software) is shown in Figure 2.

Table 1. Model rock thickness parameters and ratio.

Number	Lithology	Rock Thickness/m	Model Thickness Degree/cm	Proportion
1	Dams	15	3	100:5:3:1 (river: sand: cement: macadam: starch)
2	Loess	50	10	25:25:1:1 (river: sand: loess: petroleum jelly: solid grease)
3	Laterite	50	10	25:25:1:1 (river: sand: laterite: petroleum: jelly: solid: grease)
4	Coarse sandstone	60	12	100:5:3:2:1 (river: sand: cement: macadam: liquid: paraffin: starch)
5	Mudstone	40	8	100:5:3:2:4 (river: sand: cement: white: powder: liquid: paraffin: starch)
6	Coarse sandstone	20	4	100:5:3:2:1 (river: sand: cement: white: powder: liquid: paraffin: starch)
7	Siltstone	75	15	100:6:3:4:3 (river: sand: cement: white: powder: liquid: paraffin: starch)
8	Coarse sandstone	23	4.6	100:5:3:2:1 (river: sand: cement: white: powder: liquid: paraffin: starch)
9	Mudstone	75	15	100:5:3:2:4 (river: sand: cement: white: powder: liquid: paraffin: starch)
10	Siltstone	50	25	100:6:3:4:3 (river: sand: cement: white: powder: liquid: paraffin: starch)
11	5# Coal	9.08	4.5	20:20:1:5 (river: sand: cement: white: powder: liquid: paraffin: starch)
12	Siltstone	4	2	100:8:3:2:3 (river: sand: cement: white: powder: liquid: paraffin: starch)

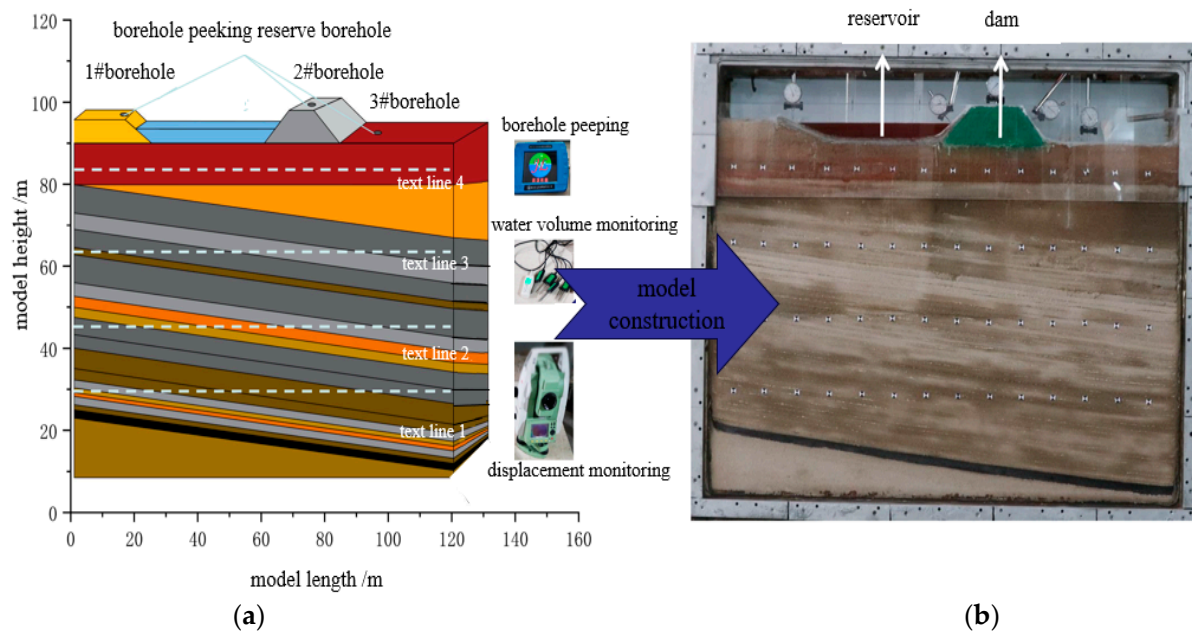


Figure 2. Physical similarity model of Wangwa Coal Mine. (a) Schematic drawing. (b) Physical drawing.

The settlement information of the model is monitored by preset measurement points on the surface of the experimental model. Specifically, a total of four rows of measuring lines from A to D were laid along the horizontal direction in the overlying rock layer of the coal seam mining, with 14 measuring points in each row, totaling 56 measuring points. The spacing of measuring points is 10 cm and the row spacing is 20 cm.

The experiment used borehole monitoring instruments to monitor the fracture development inside the model during the workings retrieval process. Three boreholes were arranged in the model, which were located at the location of the flood release area below the dam and at the junction between the surface loess layer and water at the edge of the dam and reservoir.

3.2. Overlying Rock Layers and Dam Body Rock Transport Evolution Pattern

Mining of the No. 5 coal working face in the No. 11 mining area of Wangwa coal mine caused transport damage and fracture dynamic evolution of the overlying rock layer, which posed a threat to the stability of the reservoir and the dam, thus affecting safe mining under the reservoir. Based on the mining damage theory [32–36] and through monitoring each observation point, the No. 5 coal face mining process overburden rock fall height, overburden subsidence, and surface subsidence curve were mapped out as shown in Figure 3.

As the No. 5 coal working face advances continuously, the overlying rock layer experiences pulling and cracking, direct top initial collapse, basic top breaking, and ground surface sinking. When the working face advances to 85 m from the upper coal pillar dam body level distance, the delamination phenomenon is significant, the roof rock layer collapses along the coal wall behind the formation of articulation structure, the surface movement deformation is not significant, and the surface experiences weak sinking. At 118 m, the collapse zone height no longer continues to develop upward, the overlying rock fissures are mainly horizontal fissures, the roof plate occurs larger sinking, and there is fissure zone upward development. At 148 m, the top plate collapses in a large area, the upper part of the overlying rock forms an articulated structure, the original lower part of the cladding layer gradually closes, generating new overlying rock cladding layer, and the overlying rock layer sinks but still plays a bearing role. At 175 m, because the overlying rock layer is hard, the fractures develop to a certain extent and fractures appear, the overlying rock layer sinks so that the collapse height increases, and vertical fractures

are produced at the open-cutting eye. At 200 m, the mining area is compacted, the overall bending and sinking of the rock layers mainly appear but do not expand, the amount of surface sinking increases sharply, and the sinking amount reaches 4.6 m. At 223 m, the overlying rock fissures above the working face are mainly horizontal fissures, and the fissure zone no longer continues to develop upward. Advancing toward 260 m, the overlying rock collapses in a large area, and the articulation structure is formed on the left side; the overlying rock layers sink, and the original lower part of the fissures gradually close; Due to the thicker coal seam, the overall surface subsidence is larger, forming a “concave” basin. It is found that the surface subsidence near the left and right boundaries is smaller because the boundary effect causes the left and right boundaries as the overlying rocks do not fully collapse, and the surface subsidence is the largest.

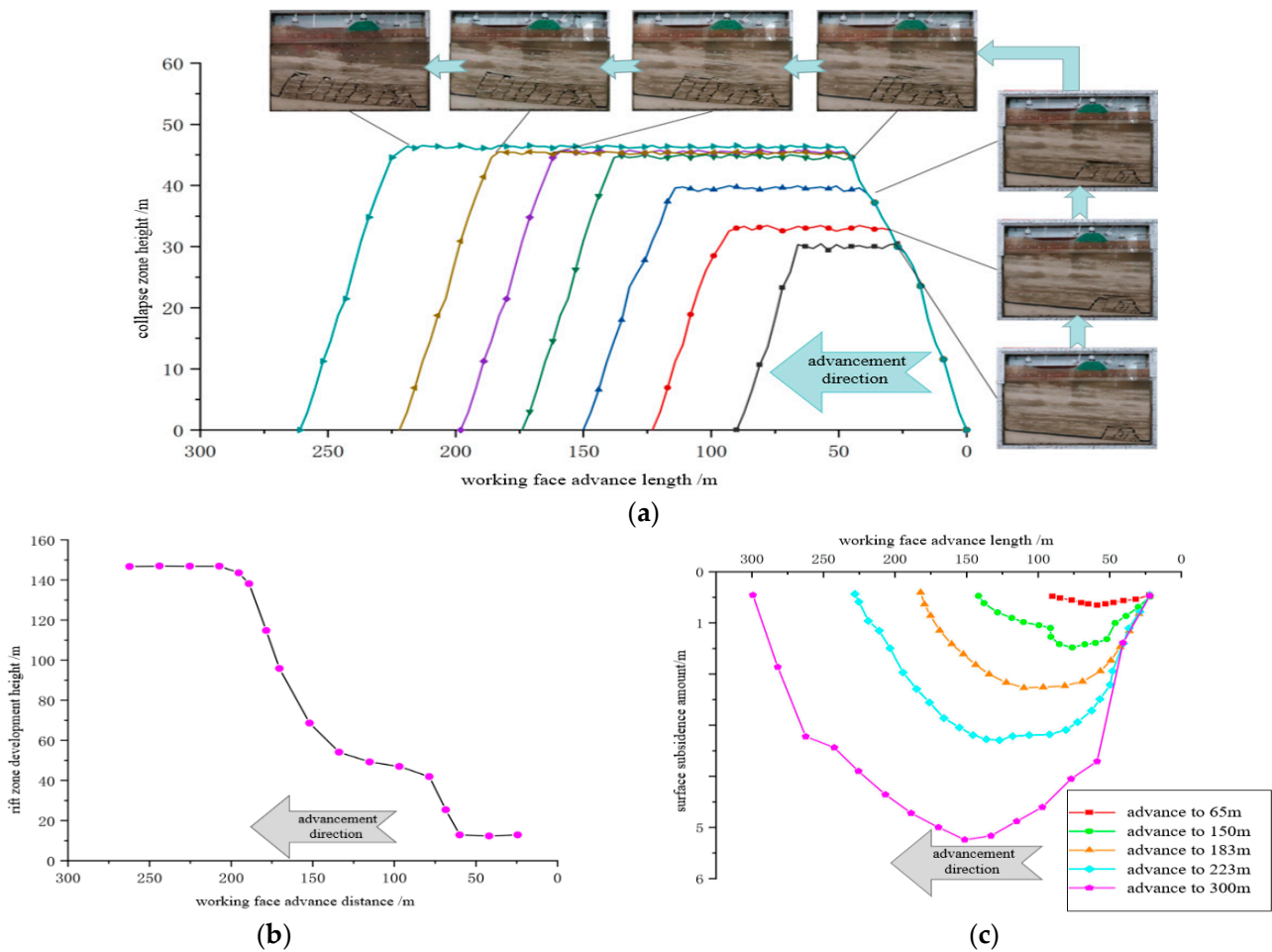


Figure 3. Overburden rock displacement curve. (a) Overlying rock collapse height. (b) Fissure zone development height. (c) Surface subsidence height.

As shown in Figure 4, after the recovery of the working surface, the distribution of the overlying rock layer collapse zone and the fracture zone is obvious, and the overlying rock collapse occurs in a large area. The height of the collapse zone is 52.4 m, the hinged structure is formed on the left side, the coal wall collapse angle is 64° , the overlying rock layer sinks, and the original lower part of the detachment gradually closes. The form of destruction is mainly the separation or cracking along the layer and the cracking or fracture of the layer vertically or obliquely. The maximum height of the collapse zone of the Wangwa coal mine is 52.4 m, and the maximum collapse ratio is 6.1, which is within the theoretical range.

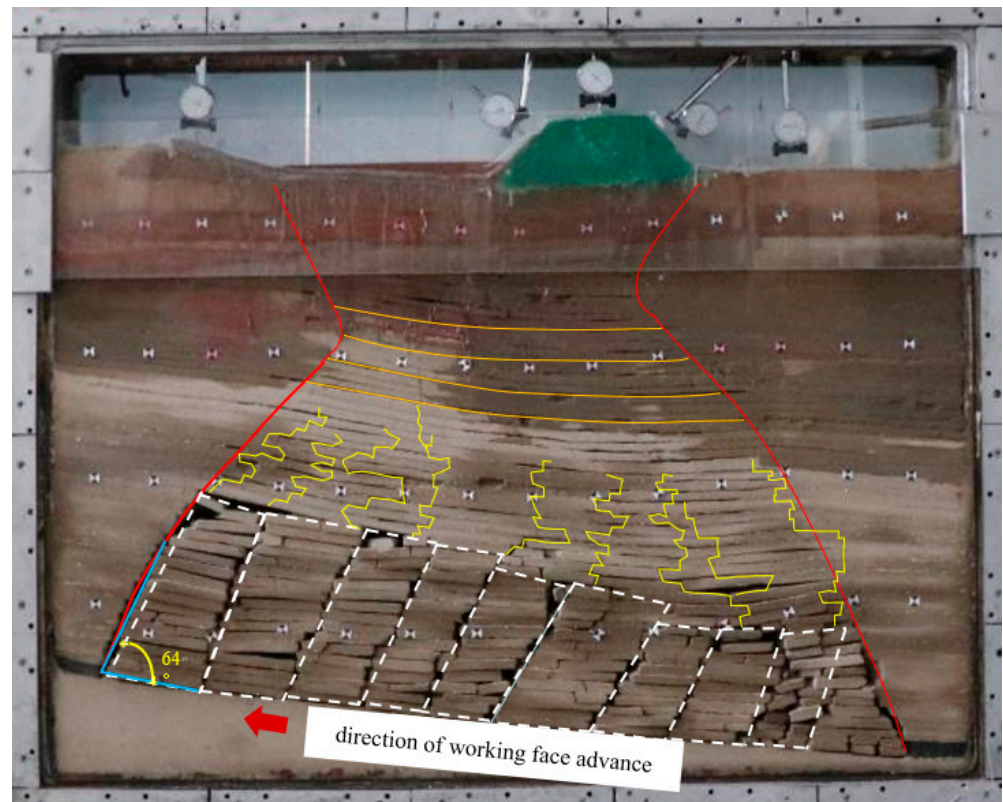


Figure 4. Overburden rock displacement after working face mining.

In the fracture zone, due to the influence of cyclic incoming pressure, the axial stretching of the overlying rock layer exceeds the limit it can withstand. The overlying rock layers exhibit evident tensile fissures that continue to spread and finally break down at the corners, causing instability, as seen by the infrared chromatograms. The rock strata near the bottom of the collapse zone are well stratified with obvious off-stratum cracking between layers. Vertical or inclined cracks are developed. In the upper part of the rock layer, the interlayer delamination cracking gradually decreases, and the multilayer combination is strengthened. The vertical cracks decrease, and most of them are microfractures occurring in the upper and lower layers of the rock layer, with few fracture cracks. The transverse and longitudinal cracks are poorly connected, and the continuity of the rock layer is relatively good.

3.3. Reservoir Water Seepage Pattern

The model water level and moisture content distribution were measured and recorded during the excavation process. The data recorded by the test process plotted the variation law of overburden moisture content with the working face advance distance, as shown in Figure 5. It can be seen from Figure 5 that the moisture content of the rock layer 50 m below the reservoir before excavation is significantly larger than that of 100 m, 200 m, and 300 m below the reservoir, which is due to the infiltration of surface water, and the moisture content of 200 m below the reservoir is smaller than that of 300 m below, which is due to the different degrees of dryness and wetness of the model before excavation. The moisture content of the overlying rock below the reservoir is on the rise with the increase of the working surface advancement distance and when the working surface advances to 178 m. The rising rate of moisture content at 50 m below the reservoir is due to the increase of surface water infiltration under the reservoir destruction. Until the excavation of the working face is completed, the moisture content of the rock layer 50 m below the reservoir is 93%, which is 60% higher than the moisture content of the rock layer before the excavation of the model, and the moisture content of the rock layer 100 m below the reservoir is 82%, which is 55% higher than the moisture content of the rock layer before

the excavation of the model. The moisture content of the rock layer 200 m and 300 m below the reservoir has not changed, which means that the surface water has not infiltrated to 200 m below the reservoir. The dynamic observation of bedrock and water barrier destruction process during the process is carried out with the help of an infrared imager. When the fracture development occurs in the observation area accompanied by energy release, the infrared imager can monitor this microscopic change and characterize the fracture field development by means of an infrared chromatogram cloud map. When the model excavation is completed, the infrared temperature chromatogram cloud map shows that the overlying rock layer is destabilized and destroyed, while the bedrock develops upward along the broken angle of about 64° . At the same time, the water level of the loose aquifer decreases, the water content tester monitors that the working face advances within the distance of 0~160 m, the water level decreases uniformly and slowly, and the moisture content rises at a faster rate of 93% at the place below the reservoir when advancing to 172 m, which is due to the destruction of the reservoir. The amount of surface water infiltration increases. The upper part of the aquifer layer produces small cracks due to tensile action, and the seepage rate of surface water to the aquifer and the diffusion on the right side of the dam body are accelerated. After the working surface is pushed to 210 m, the water level decline rate slows down due to the reclosing of the small cracks of the water barrier. In summary, it can be seen that the impact on the surface is inconsistent with the advancement of the working surface to different locations. The water level decreases from 50 mm to 12 mm after the end of the excavation of the whole model, with a decrease ratio of 76%.

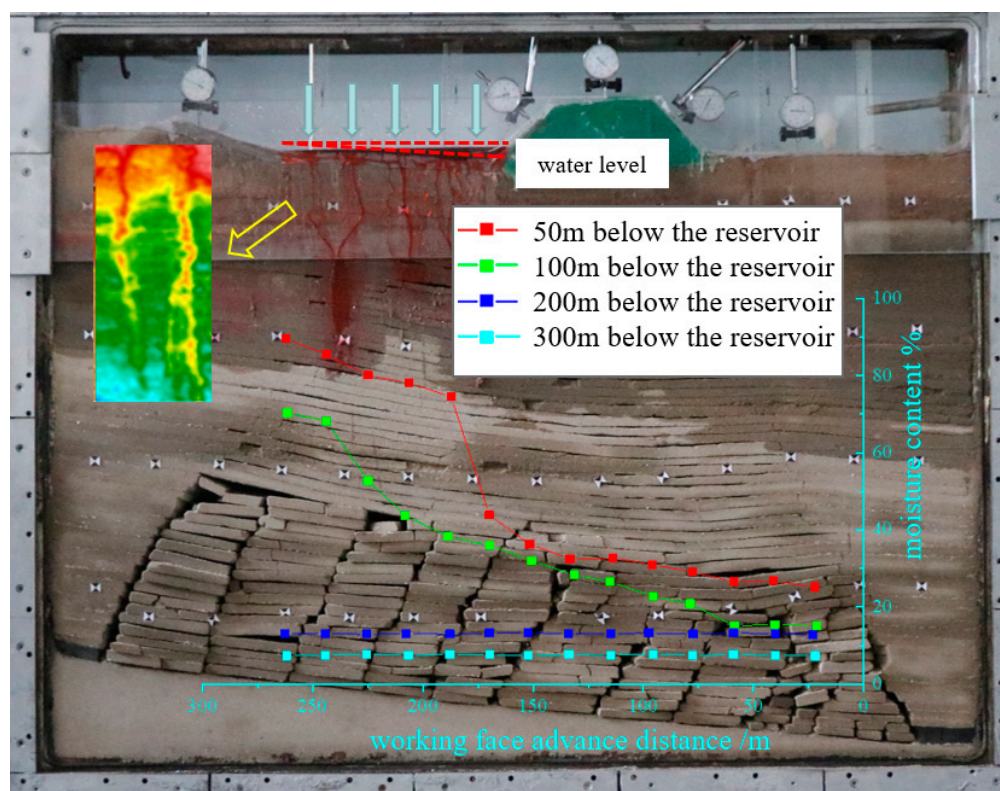


Figure 5. Moisture content variation curves of different buried depths.

3.4. Overlying Rock Fracture Development Characteristics

(1) Fracture development quantity characteristics

The fracture development of the overlying rock layer can reflect the damage of the overlying rock more intuitively after being affected by mining. In the physical simulation experiment, the fracture development inside the overlying rock was detected by using a

borehole monitor, and the supporting K-12A borehole image software was used to view and read the fracture development inside the borehole and compare it, and the number of fractures inside the borehole were plotted [37] as shown in Figure 6.

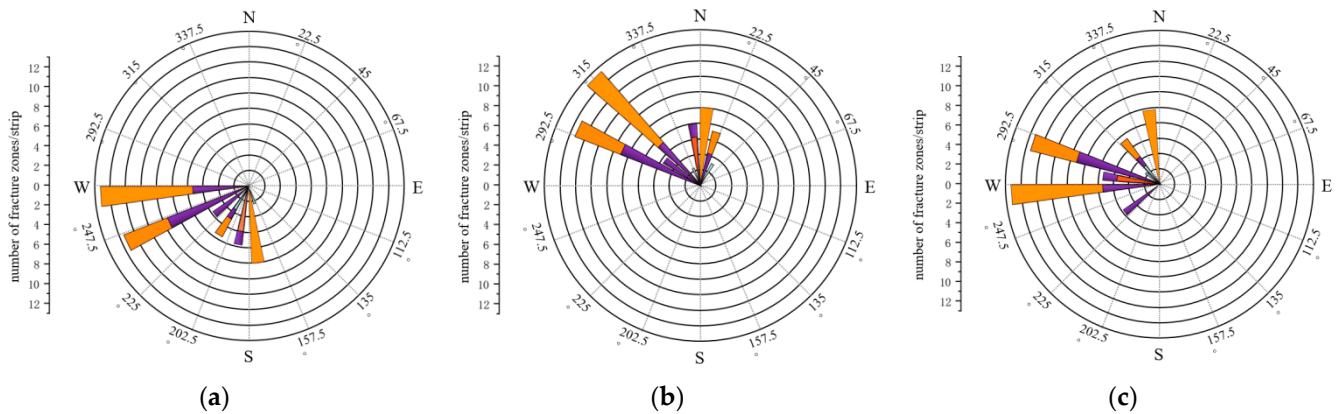


Figure 6. Azimuth rose diagram of overburden fracture development. (a) #1 drill hole. (b) #2 drill hole. (c) #3 drill hole.

After finishing the face mining, the fissure development azimuth of drill hole #1 is concentrated in the range of $170\sim 270^\circ$. The fissure development azimuth of drill hole #2 is concentrated in the range of $229.5\sim 360^\circ$ and a small amount of fissure is in the range of $0\sim 22.5^\circ$. The fissure development azimuth of drill hole #3 is concentrated in the range of $270\sim 360^\circ$. The azimuth of fracture development in drill holes #1, #2, and #3 is similar from the figure, and they are all located in the range of $180\sim 360^\circ$. In the actual production process, the mine advances from north to south. The experimental analysis suggests that the development of overburden fissures during the workings retrieval process is mainly located in the due west direction.

(2) Surface fracture development characteristics

According to the law of surface movement deformation and distribution, within the influence of mining subsidence, the surface of the peripheral area of the mining boundary of the working face is in the state of horizontal tensile deformation. When the tensile stress exceeds the tensile strength, fractures will appear on the ground surface, which is initially formed and developed in the horizontal tensile deformation zone of the ground surface at the periphery of the working face.

With the advancement of the working face, it gradually closes after transitioning to the horizontal compression deformation zone above the working face. After finishing the face mining, the reservoir water drained observed in the reservoir and the dam body to produce horizontal fissures and horizontal vertical fissures, as shown in Figure 7. In the slope of the dam body produces a 3 mm wide crack through the reservoir, fully indicating that the reservoir and the dam body will be affected by the mining disturbance. There is a certain safety hazard to the actual production, so the actual production site should do a good job of conducting the corresponding safety and waterproof measures.

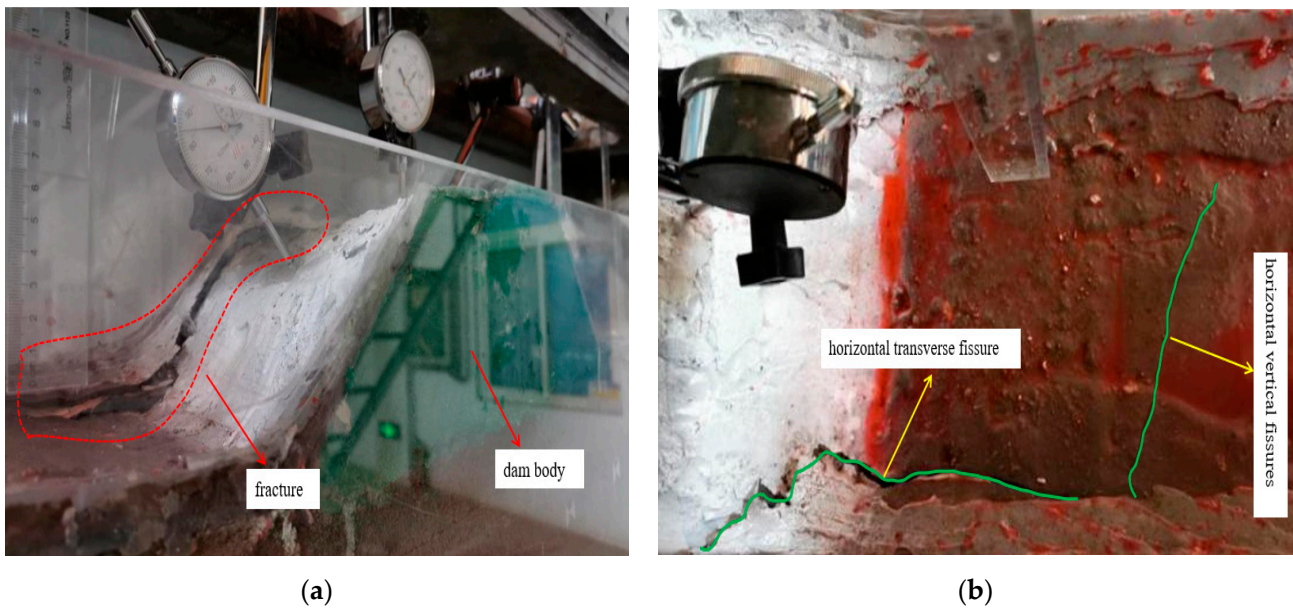


Figure 7. Characteristic map of surface movement and deformation. (a) Reservoir and dam damage map. (b) Lateral fissures in reservoir dams.

4. Simulation Analysis of Overburden Rock under Different Mining Intensity of Fracture

In order to make the observation of the spatiotemporal response law of the development of three zones with different mining intensity under the water body more intuitive, the solid–liquid coupling model was constructed relying on MIDAS and FLAC^{3D}. The following assumptions were made: the self-gravity stress field was the original stress field; the coal body after mining was treated with no water and no pressure; and the isotropic flow criterion of saturated steady flow was adopted for the fluid ontology model. The parameters such as porosity and permeability coefficient of the rock body refer to the actual measurement data of the Wangwa coal mine.

4.1. Numerical Modeling of Fluid–Solid Coupling

The Wangwa coal mine depot area under the 110,505 working face was used as a geological prototype; a three-dimensional model size of 400 m × 300 m × 450 m is established, the model is divided into 680,400 units, the height of the coal seam is 9.08 m, and the coal seam is arranged along the direction. The working face direction length is set to 300 m, and the coal seam dip angle has a selected value of 6°. The establishment of the model is shown in Figure 8. The overlying overburden of the coal seam is 423 m, and the water-bearing layer is a weak water-rich aquifer. The left, right and lower boundaries of the model are displacement fixed constraint boundaries. The upper boundary is the stress boundary, and the uniform load is applied according to the thickness of the overlying rock layer. Considering the model boundary effect, the left mining boundary is 50 m from the left boundary of the model, the right mining boundary is 50 m from the right boundary of the model, and each excavation is 10 m. According to the control chart of the upper and lower wells, the profiles are carried out along the working face direction, and the overburden plastic zone, vertical stress distribution law, overburden displacement change, horizontal displacement change, and other change laws are studied, respectively, according to the mining method after the excavation of the working face.

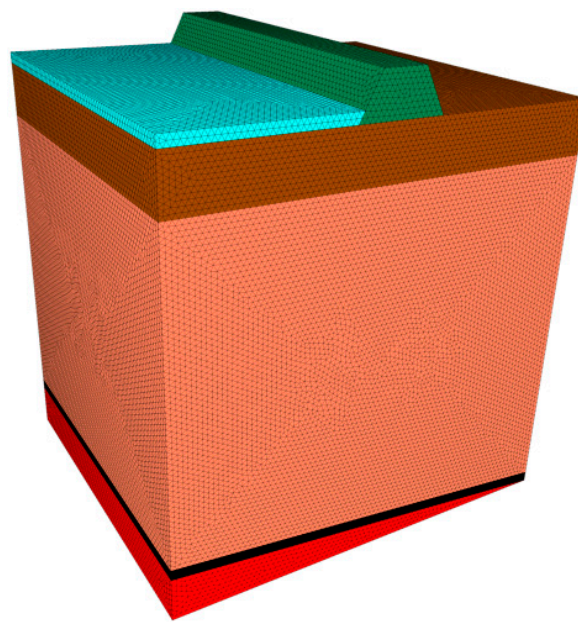


Figure 8. FLAC^{3D} numerical calculation coupling model.

4.2. Simulation Analysis of Damage Characteristics of Overlying Rock Formations

By observing the range where the overlying rock layer yielded and broke during the advancing process of the working face, the corresponding response characteristics in time and space were analyzed. In order to reflect the deformation law of the overlying rock layer more intuitively, the simulation results of the plastic zone, displacement zone, and stress zone of the overlying rock are used for analysis, the data are extracted and processed for visualization, and the calculation results are reflected in the form of a cloud diagram, as shown in Figure 9.

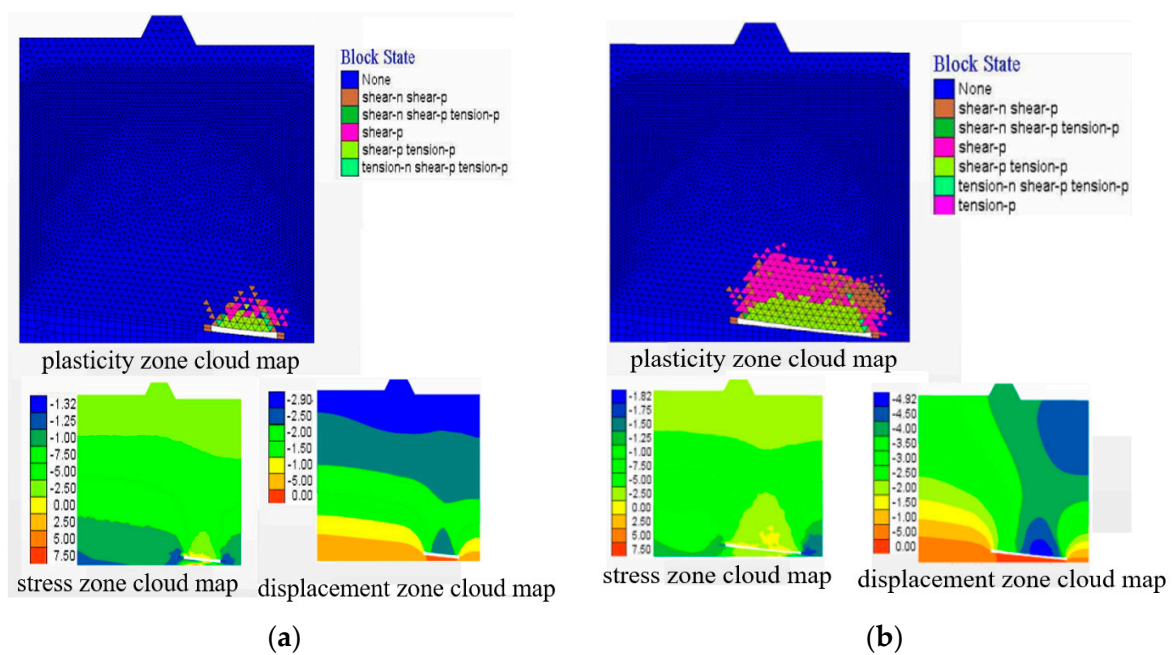


Figure 9. Cont.

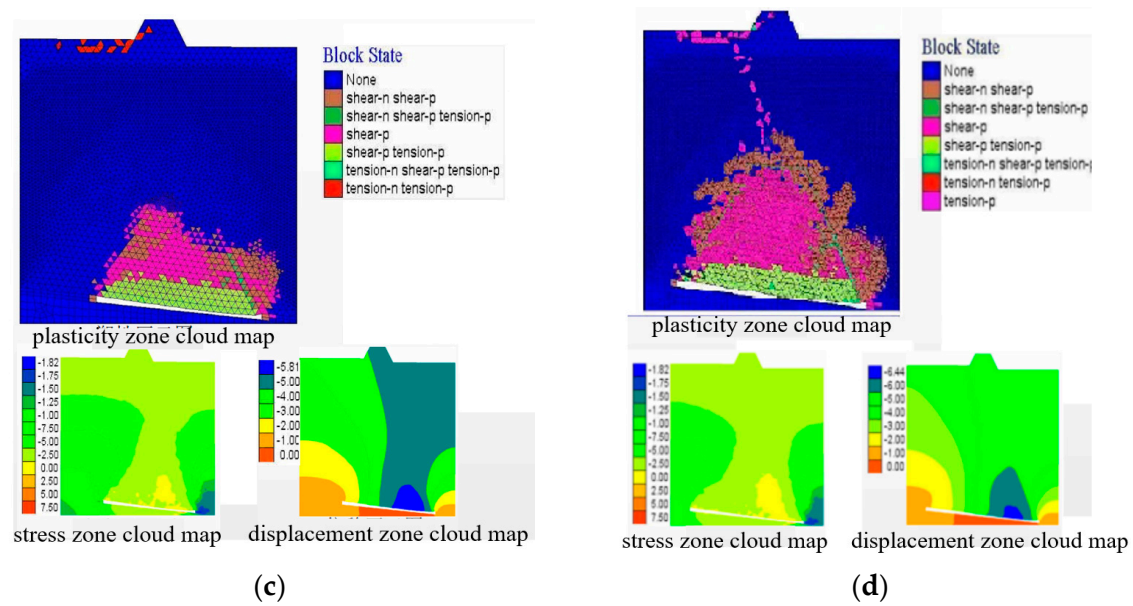


Figure 9. Failure characteristics of overlying strata with mining intensity. (a) The working face advanced to 90 m. (b) The working face advanced to 180 m. (c) The working face advanced to 240 m. (d) The working face advanced to 300 m.

From the simulation results, it can be seen that when the working face advanced to 30 m, the direct top came to pressure for the first time, which led to the central fracture, but still in the articulation state. The shear stress damage was dominant at both ends of the working face, and the plastic zone range was developed along the coal seam direction, and the broken ring range was about 8 m. Shear and tensile damage occurred in the central area, forming an inverted funnel shape, and the maximum height of the plastic zone was 24.6 m, indicating that the initial collapse of the old top had occurred. The first cycle of the old roof came to pressure and the height of the collapse zone reached 24.6 m.

When the working face advanced to 90 m, the plastic zone of the working face roof increased, the displacement diagram of the rock layer above the mining area was similar to an “arch” shape, and the surrounding rock expanded upward continuously. When the working face was advanced to 300 m, the plastic zone of overburden and pressure relief zone reached the maximum. When the working face advanced to 120 m, the old top fissure developed gradually, the top plate sinkage increased, and was irregularly collapsed. The maximum height of the overburdened plastic zone in the middle of the working face was 92 m, and the maximum height of the top plate plastic zone at the end was 53 m. The height of the collapse zone was 48 m and no longer developed, and the height of the fissure zone was 51 m. When the working face advanced to 180 m, the end of the working face was located at the left border of the dam body, the development of hydraulic fissure was larger, and the overlying rock layer was obviously bending and sinking. The overlying rock plastic zone continued to expand and was more obvious in height, showing a nearly symmetrical saddle shape; the maximum development height was located on the left side of the mining area above the oblique. When the working face advanced to 210 m, it can be seen from the figure that the top plate of the coal seam was still in the state of tensile stress damage, and the width of the damage zone in front and behind the coal wall of the working face did not change much, but the width of the plastic zone in front and behind above the mining void area had increased to 104 m. The scope of the overlying rock damage penetrated the coarse-grained sandstone in the uppermost section of the Zhiluo Group, and a smaller plastic zone appeared on the right side of the reservoir and the dam body, indicating that the mining disturbance had rippled to the reservoir and dam body, the overburden plastic zone range nearly expanded, and the plastic area continued to expand. When the working face was mined at 240 m, it is clear from the figure that the plastic zone on the left side

continued to develop upward, and the development form on the right side gradually took the shape of an arch. At this time, the shear damage was mainly distributed in the front of the coal seam advance, that is, the rear of the coal seam advance was basically stable, and the impact of mining on it was very little. When the working face was mined for 300 m, the damaged width of the front and back of the coal wall was about 15 m, and the damaged area above the coal wall on both sides of the mining area developed and connected to both ends, and new shear damage areas appeared in the upper two ends of the model. The development height of the water-conducting fractured zone was about 168 m after the mining of the working face was finished, the rock layer of Yan'an Group and Zhiluo Group above the working face was basically destroyed, and the fracture was extended to the bottom of the Anding Group, which may have a greater impact on the diving and seepage activities of the aquifer.

4.3. Development Height of Hydraulic Fracture Zone of Overburden Rock under Different Mining Height

The mining height is an important factor affecting the height of the hydraulic conductivity fracture zone, which directly influences the development height of the hydraulic conductivity fracture zone. Under the condition of keeping the thickness, burial depth, and slope length of loose layer unchanged, the height of the water-conducting rift zone development in overlying rock is studied by simulating different mining heights (2, 3, 4, 5, 6, 7, 8 and 9 m), as shown in Figure 10.

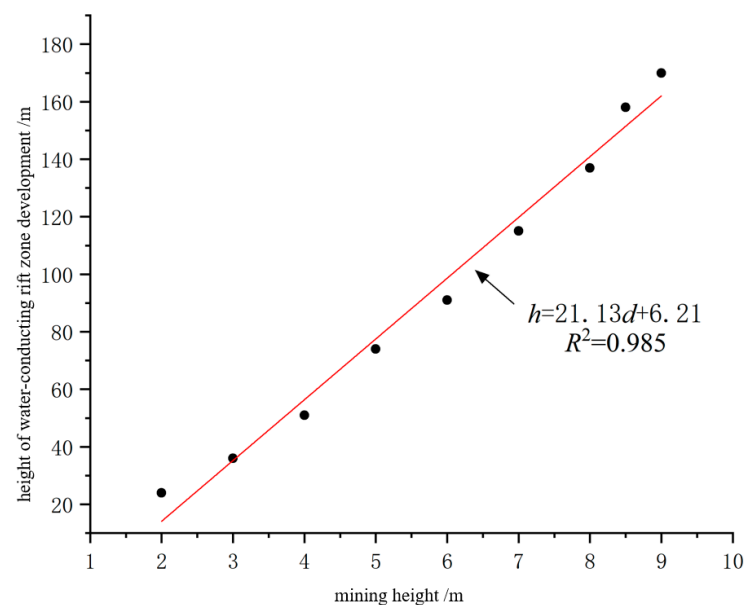


Figure 10. Height of water flowing fractured zone under different mining height.

As the mining height increases, the more space is given for the overburden to collapse. When the mining height is 2 m~3 m, the development height of the water-conducting fissure zone is 23~36 m, which is 12 times the thickness of the mining area, the direct top collapses, and the overburden around the collapsed area will be affected by tensile stress. At this time, a vertical fissure also appears; it slowly increases until there is an arch-shaped water-conducting fissure circle.

When the mining height is 4~5 m, the development height of hydraulic fracture zone is 42~58 m, which is 11 times the thickness of the mining area, the hydraulic fracture zone has been developing upward, and the off-layer fracture and longitudinal fracture are also increasing gradually. The off-layer fracture and amount are more significant when the mining height is 4~5 m than when the mining height is 2~3 m. When the mining height is 6~7 m, compared with the mining height of 2~5 m, the scope of a direct top collapse is

bigger, the overlying rock layer is affected by mining to expand the scope, and fissures start to appear in the higher rock layer. At this time, the hydraulic fissure zone has developed a height of about 90 m. When the mining height is 8~9 m, after reaching the full mining, two aspects will appear: the maximum, with the height of the hydraulic fissure zone development and the other is the amount of surface subsidence. The final development height of hydraulic fissure zone is 163 m when the mining height is 8~10 m. Through the above analysis, we can find that the development height of hydraulic fissure zone increases linearly with the increase of mining height. Therefore, as an important factor affecting the development height of hydraulic fissure zone, the mining height has an important influence on the safety of coal mining.

5. Field Measurement of Overburden Damage Height

5.1. Drill Hole Location and Program Design

Based on physical simulation and numerical simulation, the actual measurement scheme was designed to determine the overburden damage height. Two post-mining observation holes are arranged above the working face. Since the coal seam under the reservoir dam has not been mined yet, the holes are arranged in the adjacent mined working face to guide the upcoming working face.

This observation uses the drilling flushing fluid leakage method to obtain the development of hydraulic conductivity fractures in the post-mining overburden. In order to reflect the general rule of overburden damage after mining at the working face, two drill holes were drilled 285 m apart and located within the inclined centerline of the 110,503 working face, and the drill holes were arranged as shown in Figure 11.

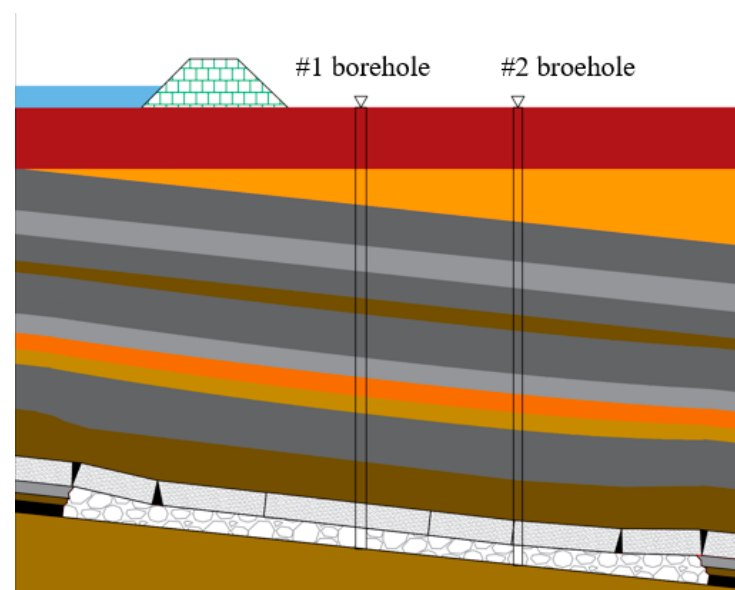


Figure 11. Working face exploration drilling arrangement.

5.2. Detection Results and Analysis

At present, the most common and accurate method for detecting the height of an overburden hydraulic fracture zone is the drill hole flushing fluid leakage method, which is used to determine the development height of an overburden hydraulic fracture zone by recording the leakage amount of flushing fluid and the change of water level in the drill hole during the drilling process. The observation of drilling flushing fluid leakage is carried out simultaneously with drilling, and the water level of the water source tank is measured when the flushing fluid forms a cycle, and the drilling depth is recorded. Thereafter, the water level of the water source tank and the hole depth of the borehole were recorded once for every 0.5 m of drilling, and the water level in the hole was recorded once for every 6 m

of drilling until the end of the observation of interruption of flushing fluid circulation, and the observation of flushing fluid leakage from the borehole was schematically shown in Figure 12.



Figure 12. Field borehole observation.

From Figure 13a, it can be seen that the amount of flushing fluid leakage starts to change at a hole depth of 267 m, and suddenly increases and enters the top of the fracture zone. The drilling is drilled to 287 m for plugging, and continues top leakage drilling after the plugging is ineffective. The hole does not return to the slurry when drilling reaches 358.60 m, when all the flushing fluid is lost. There is no water in the hole after up-drilling, and there is an significant wind absorption phenomenon in the hole. The amount of flushing fluid leakage, water level change, and abnormal phenomenon in the hole were combined, and the rock layer at a depth of 266 m was judged to be the top boundary of the fissure zone, while the top boundary of the collapse zone was judged to be 358.60 m deep.

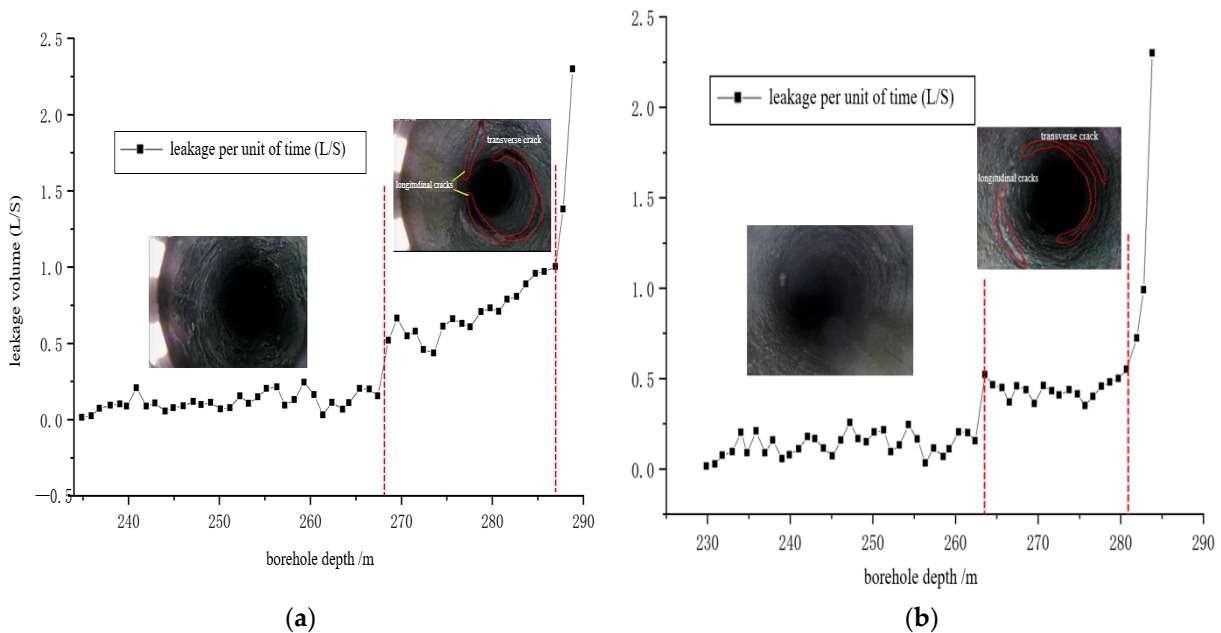


Figure 13. Field borehole observation. (a) #1 borehole leakage volume chart. (b) #2 borehole leakage volume chart.

From Figure 13b, it can be seen that when drilling to 262 m, the flushing fluid leakage was interrupted and gradually increased, and at 283 m deep, all flushing fluid was lost, and no water was returned after repeated water injection tests. In order to investigate the

height of the collapse zone, we drilled to the hole depth of 382.90 m when all the flushing fluid was lost and decided that this was the top boundary of the collapse zone.

According to the geological record of the core and the borehole observation, the position of the top interface of the fissure zone development is approximately 234.85 m in the depth of Hole No. 1, and the height of the water-conducting fissure zone development is 161.15 m, which is 17.9 times the mining thickness. The location of the top interface of the collapse zone is around 352 m deep in Hole No. 1, the height of the collapse zone is 39.85 m, and the collapse ratio is 4.4. The location of the top interface of the fracture zone development in Hole No. 2 is around 253.8 m deep, the height of the water-conducting fracture zone development is 170.76 m, which is 19 times of the mining thickness, and the location of the top interface of the collapse zone is around 225.24 m deep in Hole No. 2. The height of the collapse zone is 47.76 m, and the ratio of collapse to mining is 5.3; the development height of the No. 5 coal bending and sinking zone has reached the surface, and the surface is subject to uneven settlement to produce tensile fissures.

5.3. Three-Band Height Formula Correction Analysis

Since the physical simulation and numerical simulation are already simplifying the relevant geological conditions, there are deviations between their obtained data and the actual data in the field. Therefore, in order to obtain more accurate research data, based on the above comprehensive analysis, four groups of data from similar physical simulation experiments, numerical simulation experiments, empirical formula analysis and field actual measurements are compared with the measured maximum value: the height of the collapse zone is 47.76 m, and the height of the water-conducting fracture zone development is 170.76 m. We refer to the empirical formula derived from a study by Jianshi Zhang [38]:

$$H_m = \frac{100\sum M}{0.49\sum M + 19.12} \pm 4.17 \quad (1)$$

$$H_{li} = \frac{100\sum M}{0.23\sum M + 6.10} \pm 10.42 \quad (2)$$

where: H_m is the height of collapse zone, H_{li} is the height of hydraulic fracture zone, and M is the thickness of coal seam mining, take 9 m.

According to the formula of the height of the hydraulic fracture zone, the height of the overlying rock collapse zone in the mining area is 34.07~42.42 m, respectively; and the height of the fracture zone development is 99.74~120.57 m. In the process of using downhole quantitative detection, the amount of water injection leakage within this height should be focused on observation.

The experimental observations and the values calculated by the empirical formula are now compared and analyzed as shown in Table 2.

Table 2. Comparison of two-band heights under different methods.

Method Classification	Overburden Damage Height/m		Error/%	
	Collapse Zone	Water-Conducting Fissure Zone	Collapse Zone	Water-Conducting Fissure Zone
Physical Simulation	52.4	162	+9.72	−5.13
Numerical Simulation	48.11	164	+0.73	−3.96
Empirical formulas	42.42	120.57	−11.18	−29.39
Field measurements	47.76	170.76	0	0

As shown in Table 2, the height of the hydraulic fracture zone calculated by empirical formula has a large error of −29.39% with the field measurement results. According to the calculation results in Table 2, because the field observation results of the development height of hydraulic fissure zone of mining overburden differ greatly from the calculation results of the empirical formula, and the development height of the hydraulic fissure zone of the mining working face is not clear, for the sake of safety, the maximum field observation

data, taken as the height of hydraulic fissure zone under the conditions of this mine, the height of the collapse zone and the height of the hydraulic fracture zone of the traditional “three under mining” (abbreviation for coal mining under water bodies, under buildings and under railroads.) specification empirical formula are both expected to be significantly lower than the measured values. There will be certain safety risks if the relevant safety regulations are formulated in this way, while the prediction model of similar simulation experiments, numerical simulation and the actual measured values in the field are in good agreement, with an error of less than 5%. Therefore, the traditional empirical formula of the “three under mining” specification is optimized by using the variance coefficient to meet the actual needs of production mines. The standard deviation theory is applied to analyze the height of the hydraulic fracture zone and the height of the collapse zone, namely:

$$\sigma = \sqrt{\frac{\sum_{i=1}^n (x_i - \bar{x})^2}{n}} \quad (3)$$

where: \bar{x} is the average of the data. The root mean square error of the collapse zone and the hydraulic fracture zone of the Wangwa coal mine No. 11 mining area are 7.86 and 20.01, respectively, by substituting the data obtained from the above four methods into Equation (4). The variance correction coefficient is brought into the empirical formula to obtain the hydraulic fracture zone correction formula applicable to high-intensity mining under the dam of the reservoir in the western ecologically fragile area:

$$H_{ms} = \frac{100\sum M}{(0.49\sum M + 19.12)k} \pm 4.17 \quad (4)$$

$$H_{lis} = \frac{100\sum M}{(0.26\sum M + 6.88)k} \pm 11.49 \quad (5)$$

where: H_{ms} is the correction working face collapse zone height; H_{lis} is the correction working face hydraulic fracture zone height; $\sum M$ is the cumulative mining thickness of coal seam; and k is the variance correction coefficient.

In summary, under the condition of thick coal seam comprehensive discharge mining under the reservoir dam body, the overlying rock layer water conductive fracture zone penetrates to the surface, resulting in downward leakage of reservoir water and causing damage to the reservoir dam body, which causes loss to the local ecological environment and agricultural development. Thus, it is necessary to reduce the impact of underground mining disturbance on the surface and other methods for economic analysis. ① Currently infill mining, as an important method of green mining at this stage, has a wide range of applications. However, because the No. 11 mining area working face of the Wangwa coal mine is located under the dam of the reservoir, it leads to the engineering difficulty of filling materials from the ground borehole into the mining area. When laying pipes from underground, it indirectly causes the production cost of the mine to increase, so it is not applicable to the mine. ② Moving and Pouring Face is the simplest method to deal with the problem of coal seam mining under complex geological conditions due to the strict management of coal resources at this stage of the country. In order to avoid the waste of coal resources and coal mines that generate economic loss, this method may not be used as a mining method that does not add extra cost. ③ Limited height mining ensures the safety of coal mines and the safety of workers on the basis of ensuring the safe production of coal mines. It can effectively reduce the water-conducting fissure zone through to the surface, resulting in surface water influx to the working face of the flooded wells, so as to achieve the purpose of green mining.

Through the field observation of the leakage amount of the borehole, it is known that the height of the hydraulic fissure zone development is 170.76 m. The development to the sub-clay water barrier layer below, and the reservoir dam body deformation damage,

after physical simulation simulation experiments to get the bending subsidence zone above the water barrier layer, and by the mining height of the influence of the obvious. In order to avoid the water seepage into the ground from the dam and reservoir area due to the excessive mining height in the actual production process, the development height of the water-conducting fissure zone should not be similar to the water-insulating soil layer. According to the experimental results, the safe height of the water-conducting fissure zone is controlled at 82.88 m, which is reintroduced into the correction Formula (5). The back calculation shows that when the safe mining height of the working face is 2.6~4.2 m, the development range of water-conducting fissure zone can be controlled at a safe height. That is, when the mining height is reduced to 2.6 m, the water barrier under the reservoir water body can be in a stable and continuous state. This can ensure the safety and stability of the reservoir water body, reduce the large deformation of the ground dam caused by underground mining and the reservoir water gushing into the working face, reduce the incidence of flooding accidents, and ensure the safe production of the mine.

According to the “Three Underground Coal Mining Regulations”, “Technical Specification for Water Conservation Coal Mining” (and the “Design Specification for Embankment Project Management”, combined with the above correction results of the three belt heights of the mine, this research provides a reference on the management of coal mining collapses under lakes and rivers in China. Therefore, at this stage, using the method of limiting the mining height to 2.6 m keeping the original working face equipment unchanged, reducing the mining height of the coal seam can effectively avoid damage to the dam and the water body due to mining disturbances. At the same time, engineering and technical measures such as pre-raising the dam, grouting, and seepage control have been taken to ensure the safe recovery of the coal mine. Up to now, the working face under the reservoir dam of the Wangwa coal mine has been safely mined. During the period of mining, the water volume of the reservoir is stable, and the water consumption of the working face is always within the safe water influx threshold of $94 \text{ m}^3/\text{h}$. This indicates that the safety of high-intensity mining under the water body can be greatly improved by accurate correction prediction of the guide height zone.

6. Conclusions

By analyzing the rock assignment of the No. 5 coal seam, geological structure and hydrogeological data of the Wangwa coal mine, physical simulation, numerical simulation and theoretical analysis were used to study the prediction of safety under the reservoir dam of the Wangwa coal mine, and the following main conclusions were reached:

- (1) Based on the solid–liquid coupling test platform, the development of cracks inside the model during the working face mining process is monitored through physical simulation experiments using a borehole monitoring instrument. The experiment concluded that when the tensile stress exceeds the tensile strength, cracks will appear on the surface. The seepage of the water body of the reservoir is inconsistent with the working face advancing to different positions on the surface, and the reservoir and the dam body will be affected by the mining disturbances during the mining process, which will lead to cracks and trigger the problem of sudden water flow. Therefore, appropriate safety and waterproofing measures should be taken in the actual production of the site.
- (2) Through the numerical model of fluid–solid coupling, the development height of hydraulic fracture zone increases linearly with the increase of mining height. Therefore, mining height is an important factor affecting it. The height of water-conducting fissure zone is not the same in Northwest China due to the different conditions of coal seams, so the authenticity and practicality of the traditional “three lower mining” standard empirical formula will be greatly reduced in this case. In order to ensure the accuracy of the data, the physical simulation experiment, numerical calculation, and traditional empirical formula are compared, to arrive at 162 m, 164 m, and 120.57 m

of hydraulic fracture zone height, respectively, among which the calculation results of the empirical formula are different and need further correction.

- (3) Through the on-site monitoring of the amount of leakage in the borehole, the measured data are obtained from the borehole TV and the traditional empirical formula for the height of the hydraulic fissure zone data for comparison. The error between the two is as high as -29.39% , which will seriously affect the decision of the site water control work. In this case, an accurate correction of the empirical formula was made to reduce the error value between the empirical formula and the actual measurement. On this basis, for the protection of surface buildings and water bodies, the coal seam mining height of 2.6 m was reversed to ensure safe production as much as possible, and the resources under the water bodies were retrieved as much as possible. In addition, the same geological conditions exist around the Wangwa Mine, which provides a basis for decision-making for similar mines in the vicinity.

Author Contributions: T.Y. and J.D. conceived and designed the experiments; B.P. and J.Z. analyzed the data; T.Y., Y.Z., Y.Y. and J.Z. wrote the paper. All authors have read and agreed to the published version of the manuscript.

Funding: This study was supported by the National Natural Science Foundation of China (no. 52004200).

Data Availability Statement: All data generated or analyzed during this study are included in this article.

Acknowledgments: This study was supported by the National Natural Science Foundation of China (no. 52004200), The agency's funding is gratefully acknowledged.

Conflicts of Interest: The authors declare no conflict of interest.

References

1. National Bureau of Statistics of the People's Republic of China. *China Statistical Yearbook Beijing*; China Statistics Press: Beijing, China, 2020.
2. Liu, G.; Wang, Y.; Gao, C.; Tian, G. Feasibility analysis of multiple coal seams mining under reservoir and dam. *Coal Sci. Technol.* **2020**, *48*, 185–191.
3. Zeng, Y.; Wu, Q.; Zhao, S.; Tian, Y.; Zhang, Y.; Mei, O.; Meng, S. Characteristics, causes, and prevention measures of coal mine water hazard accidents in China. *Coal Sci. Technol.* **2023**, *10*, 22. [[CrossRef](#)] [[PubMed](#)]
4. National Development and Reform Commission; National Energy Administration. *Development Plan of Mine Water Utilization*; National Development and Reform Commission: Beijing, China, 2013.
5. Ministry of Environmental Protection. *Water Pollution Prevention and Control Action Plan: Chinese and English*; People's Publishing House: Beijing, China, 2015.
6. Wu, Q.; Shen, J.; Wang, Y. Mining techniques and engineering application for "Coal-Water" dual-resources mine. *J. China Coal Soc.* **2017**, *42*, 8–16.
7. Cao, Z.; Ju, J.; Xu, J. Distribution model of water-conducted fracture main channel and its flow characteristics. *J. China Coal Soc.* **2019**, *44*, 3719–3728.
8. Cao, Z.; Li, Q.; Dong, B. Water Resource Protection and Utilization Technology and Application of Coal Mining in Shandong Mining Area. *Coal Eng.* **2014**, *46*, 162–164+168.
9. Wu, Q.; Li, D. Research of "Coal-water" double-resources mine construction and development. *China Coal Geol.* **2009**, *21*, 32–35+62.
10. Wang, S.; Huang, Q.; Fan, L.; Yang, Z.; Shen, T. Study on overburden aquiclude and water protection mining regionalization in the ecological fragile mining area. *J. China Coal Soc.* **2010**, *35*, 7–14.
11. Wang, S. Thoughts about the main energy status of coal and green mining in China. *China Coal* **2020**, *46*, 11–16.
12. Wang, S.; Shen, Y.; Song, S.; Liu, L.; Gu, L.; Wei, J. Change of coal energy status and green and low-carbon development under the "dual carbon" goal. *J. China Coal Soc.* **2023**. [[CrossRef](#)]
13. Fan, L. Development of coal mining method with water protection in fragile ecological region. *J. Liaoning Tech. Univ.* **2011**, *30*, 667–671.
14. Fan, L.; Ma, X.; Ji, R. Progress in engineering practice of water-preserved coal mining in the Western eco-environment frangible area. *J. China Coal Soc.* **2015**, *40*, 1711–1717.
15. Fan, L.; Wu, Q.; Peng, J.; Chi, B.; Sun, K.; Wang, H.; Guo, Z.; Ning, K.; Liu, S.; Li, C.; et al. Thoughts and methods of geological environment monitoring for large coal bases in the middle reaches of the Yellow River. *J. China Coal Soc.* **2021**, *46*, 1417–1427.

16. Huang, Q. Impermeability of Overburden Rock In Shallow Buried Coal Seam And Classification Of Water Conservation Mining. *J. Rock Mech. Eng.* **2010**, *29* (Suppl. 2), 3622–3627.
17. Huang, Q.; Zhang, W.; Hou, Z. Study of Simulation Materials of Aquifuge For Solid-Liquid Coupling. *J. Rock Mech. Eng.* **2010**, *29* (Suppl. 1), 2813–2818.
18. Huang, Q. Progress and prospect of rock formation control for safe and green mining in large shallow-buried coalfields in the west. *J. Xi'an Univ. Sci. Technol.* **2021**, *41*, 382.
19. Chi, M. Evaluation of Water Resources Carrying Capacity and Decision-Making of Scientific Mining Scale in the Northwest Mining Area of China. Ph.D. Thesis, China University of Mining and Technology, Xuzhou, China, 2019.
20. Zhang, J.; Hou, Z. Study on Three Strap in Water Resouces Preservation in Yu-shu-wan Shallow Seam Mining. *J. Hunan Univ. Sci. Technol.* **2006**, 10–13.
21. Lai, X.; Cui, F.; Cao, J.; Lv, Z.; Kang, Y. Analysis on characteristics of overlying rock caving and fissure conductive water in top-coal caving working face at three soft coal seam. *J. Coal* **2017**, *42*, 148–154.
22. Gale, W. Review and estimation of the hydraulic conductivity of the overburden above longwall panels. Experience from Australia. In Proceedings of the 19th International Conference on Ground Control in Mining, Morgantown, WV, USA, 8–10 August 2010; pp. 1–8.
23. Tiwary, R.K. Environmental Impact of Coal Mining on Water Regime and Its Management. *Water Air Soil Pollut.* **2001**, *132*, 185–199. [[CrossRef](#)]
24. State Administration of Safety Supervision; State Administration of Coal Mine Safety; National Energy Administration. *Specification for Coal Pillar Retention and Coal Compression Mining for Buildings, Water Bodies, Railroads and Major Shafts*; Coal Industry Press: Beijing, China, 2017.
25. Hu, B.N.; Zhang, H.X.; Shen, B.H. *Guide to Coal Pillar Retention and Coal Compression Mining for Buildings, Water Bodies, Railroads and Major Shafts*; Coal Industry Press: Beijing, China, 2017.
26. Mokhov, A.V. A rock mass permeability model within the subsidence zone in workings of coal fields. *Dokl. Earth Sci.* **2017**, *473*, 390–393. [[CrossRef](#)]
27. Xue, S.; Wu, X.; Xu, N. Pondering on Coal Mining under Large-sized Reservoir Research. *Coal Geol. China* **2008**, *20* (Suppl. 1), 47–49.
28. Zhang, J.; Yang, T.; Suo, Y.; Liu, D.; Zhou, F. Roof water-inrush disaster forecast based on the model of aquiclude instability. *J. Coal* **2017**, *42*, 2718–2724.
29. Lai, X.; Xu, H.; Fan, J.; Wang, Z.; Yan, Z.; Shan, P.; Ren, J.; Zhang, S.; Yang, Y.; Zhou, Z. Study on the mechanism and control of rock burst of 2 coal pillar under complex conditions. *Geofluids* **2020**, *2020*, 8847003. [[CrossRef](#)]
30. Hou, Z.; Zhang, J. Experiment and analysis of diving protection solid-liquid two-phase coupling in mining area of northern Shaanxi Province. *J. Hunan Univ. Sci. Technol.* **2004**, *19*, 1–5.
31. Zhang, J.; Yu, X.; Cheng, L. Failure mechanism of soil layer in longwall face intermission advance in shallow seam mining. *J. Liaoning Tech. Univ.* **2008**, *27*, 801–804.
32. Zhang, J.; Yang, T.; Suo, Y.; Sun, Y.; Cai, W.; Liu, Q. *Forecast Model for Roof Water Inrush in Anshan Coal Mine Based on Coupling Evaluation*; Xi'an University of Science and Technology: Xi'an, China, 2018; Volume 38, pp. 569–576.
33. Eremin, M.; Esterhuizen, G.; Smolin, I. Numerical simulation of roof cavings in several Kuzbass mines using finite-difference continuum damage mechanics approach. *Int. J. Min. Sci. Technol.* **2020**, *30*, 157–166. [[CrossRef](#)]
34. Kwinta, A.; Gradka, R. Analysis of the damage influence range generated by underground mining. *Int. J. Rock Mech. Min. Sci.* **2020**, *128*, 104263. [[CrossRef](#)]
35. Lai, X.; Sun, H.; Shan, P.; Wang, C.; Cui, N.; Yang, Y. Acoustic emission and temperature variation in failure process of hard rock pillars sandwiched between thick coal seams of extremely steep. *Chin. J. Rock Mech. Eng.* **2015**, *34*, 2285–2292.
36. Dai, Z.; Tang, J.; Wang, Y.; Jiang, Z.; Zhang, L.; Liu, S. A model for predicting mining subsidence in bedding rock slopes. *Chin. J. Rock Mech. Eng.* **2017**, *36*, 3012–3020.
37. Lai, X.; Zhang, X.; Shan, P.; Cui, F.; Liu, B.; Bai, R. Study on development law of water-conducting fractures in overlying strata of three soft coal seam mining under thick loose layers. *Chin. J. Rock Mech. Eng.* **2021**, *40*, 1739–1750.
38. Zhang, J.S. Overview of empirical formulas for predicting the development height of hydraulic fracture zones in coal mining. *Min. Technol.* **2018**, *18*, 86–88+110. [[CrossRef](#)]

Disclaimer/Publisher's Note: The statements, opinions and data contained in all publications are solely those of the individual author(s) and contributor(s) and not of MDPI and/or the editor(s). MDPI and/or the editor(s) disclaim responsibility for any injury to people or property resulting from any ideas, methods, instructions or products referred to in the content.